

Fast Digital Tomosynthesis for LIVE Radiation Therapy

GTC 2015 – San Jose, CA, USA



Alexandros-Stavros Iliopoulos¹



Nikos Pitsianis^{2,1}



Xiaobai Sun¹



Fang-Fang Yin³



Lei Ren³

¹Department of Computer Science, Duke University

²Department of Electrical and Computer Engineering, Aristotle University of Thessaloniki

³Department of Radiation Oncology, Duke University School of Medicine

March 19, 2015

Outline

- 1 Introduction: IGRT & LIVE
- 2 Cone-beam operators
- 3 Experiments
- 4 Discussion
- 5 Acknowledgements

Outline

1 Introduction: IGRT & LIVE

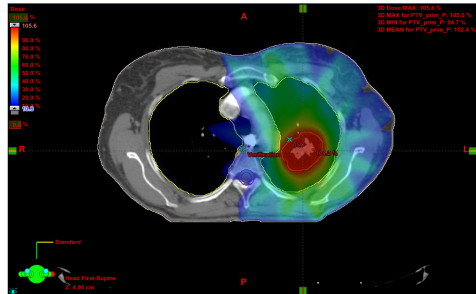
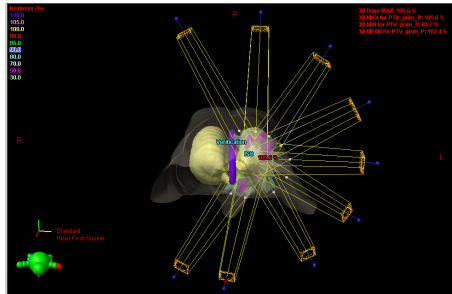
2 Cone-beam operators

3 Experiments

4 Discussion

5 Acknowledgements

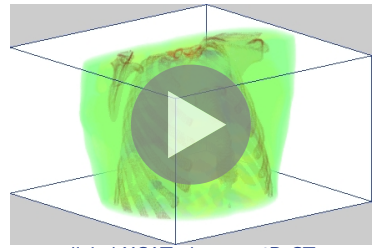
Image-guided radiation therapy (IGRT)



- Highly focused radiation delivery
 - Can eliminate early-stage cancer
 - Accurate targeting is critical
- Volumetric imaging information
 - Pre-treatment planning (above)
 - ★ On-board target verification during treatment
 - Post-evaluation

Image-guided radiation therapy: challenges

- Dynamic deformation:¹
 - Intrafraction (respiration, etc)
 - Tumor displacement, growth/shrinkage
 - Deviates from planning data
 - Hampers targeting precision
 - Complicates projection registration
- Clinical considerations for on-board imaging:^{2,3}
 - Low dose
 - Rapid acquisition
 - ★ High-fidelity, fast digital processing



(plus tissue deformation for real body)

¹Redmond et al. *IJROBP* (75), 2009

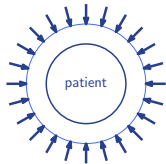
²Maurer et al. *Medical Physics* (37), 2010

³Ren et al. *Medical Physics* (41), 2014

Digital Tomosynthesis (DTS) with LIVE

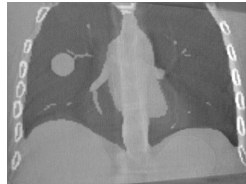
acquisition

CBCT (full scan)

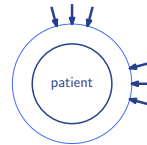


scan angle: $360^\circ / \sim 200^\circ$
scan time: ~ 1 min
scan dose: $1 \sim 8$ cGy

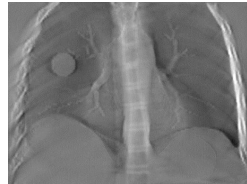
reconstruction slice



DTS (limited-angle scan)



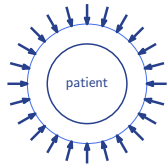
scan angle: $20^\circ \sim 60^\circ$
scan time: < 10 sec
scan dose: ≤ 1 cGy



Digital Tomosynthesis (DTS) with LIVE

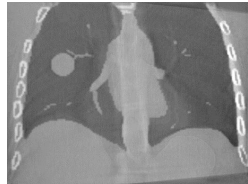
acquisition

CBCT (full scan)

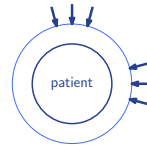


scan angle: $360^\circ / \sim 200^\circ$
scan time: ~ 1 min
scan dose: $1 \sim 8$ cGy

reconstruction slice



DTS (limited-angle scan)



scan angle: $20^\circ \sim 60^\circ$
scan time: < 10 sec
scan dose: ≤ 1 cGy



LIVE goal

LIVE overview

- Purpose: High-fidelity reconstruction of dynamic volume from limited-angle on-board projections
 - LIVE is the first prototype of its kind
- Key idea:
 - Use 4D planning CT as prior data
 - Model on-board volume as deformation of prior CT
- Methods:
 - Prior respiratory motion model + free-form (voxel-wise) deformation field
 - Complementary kV-MV projections
 - ★ Iterative deformable registration (computation-intensive)

Ren et al. IJROBP (82), 2012

Zhang et al. Medical Physics (40), 2013

Ren et al. Medical Physics (41), 2014

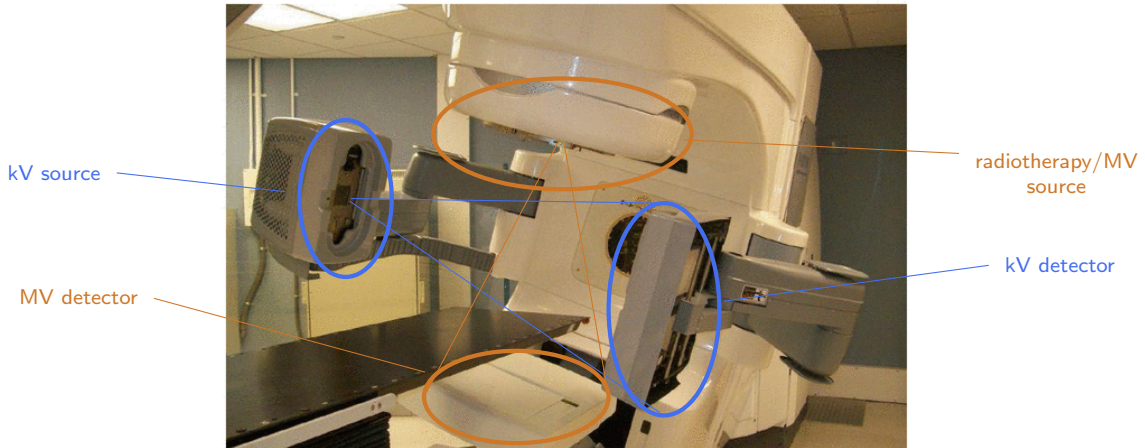
LIVE imaging/therapy system



One of the radiosurgery systems at Duke (Novalis Tx)¹

¹Chang et al. JACMP (33), 2012

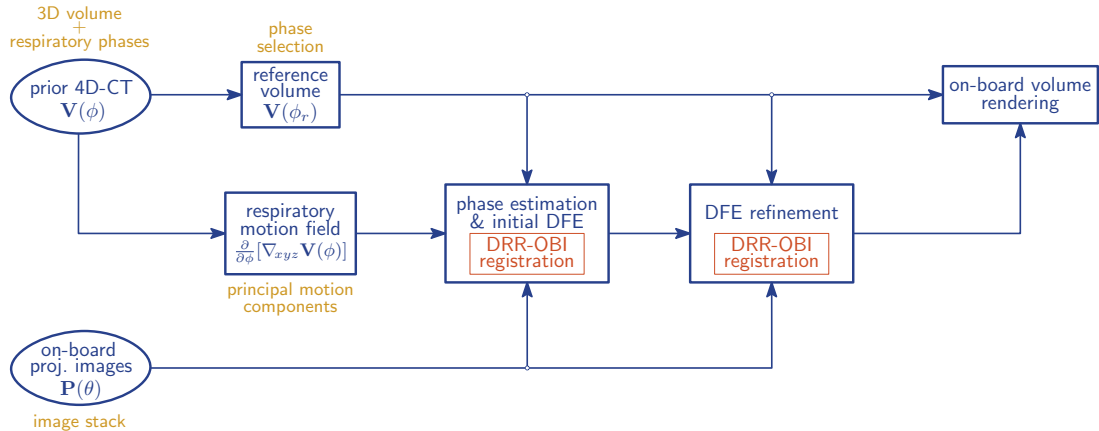
LIVE imaging/therapy system



One of the radiosurgery systems at Duke (Novalis Tx)¹

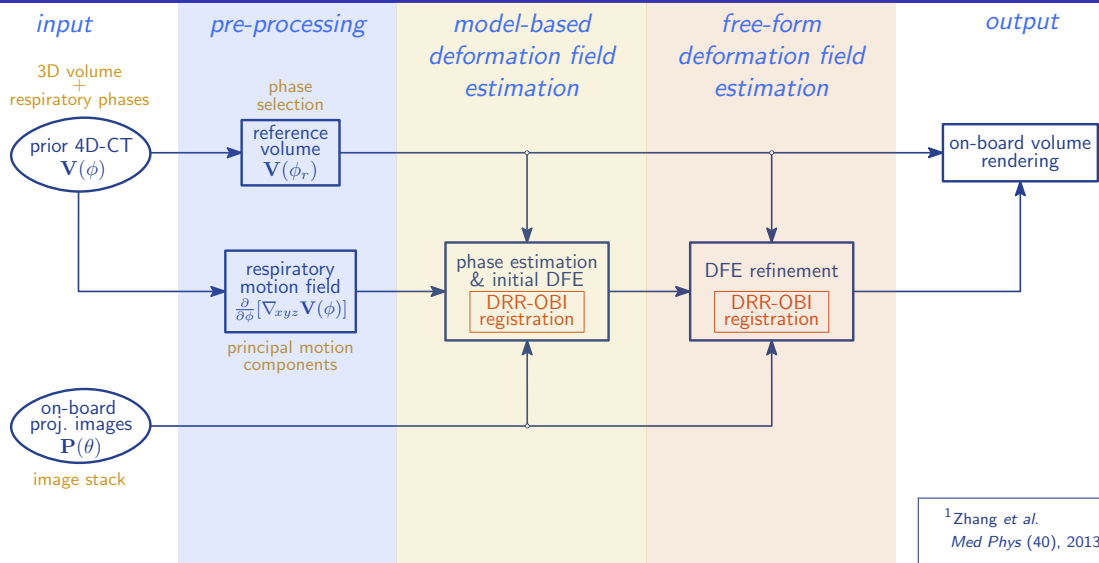
¹Chang et al. JACMP (33), 2012

LIVE DTS algorithm¹



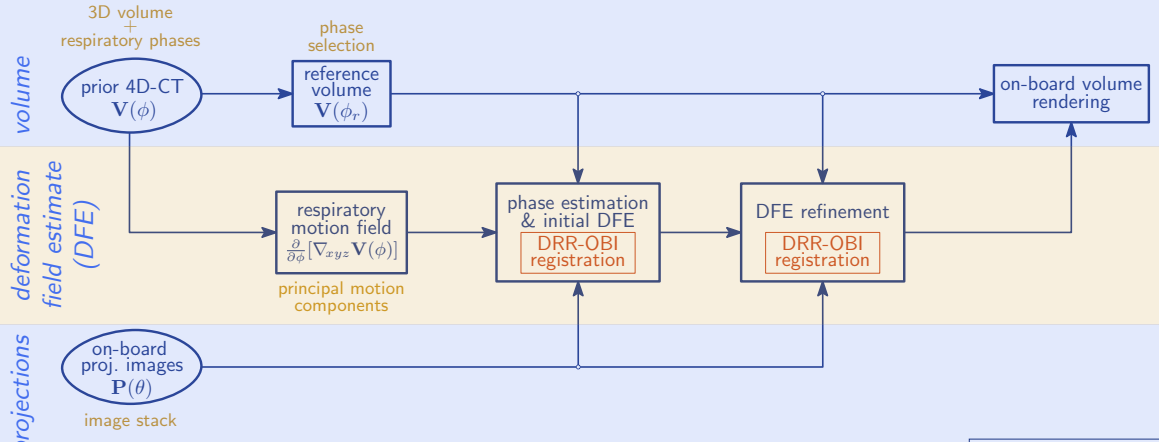
¹Zhang et al.
Med Phys (40), 2013

LIVE DTS algorithm¹



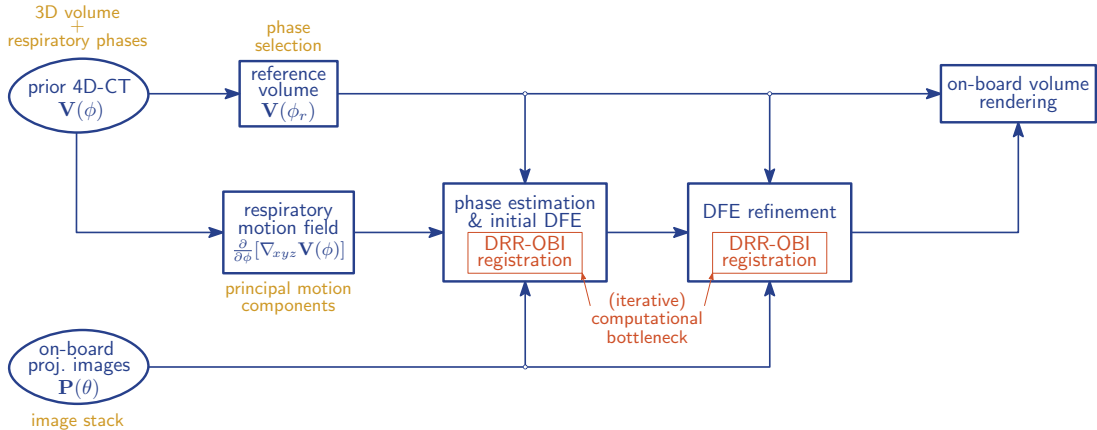
¹Zhang et al.
Med Phys (40), 2013

LIVE DTS algorithm¹



¹Zhang et al.
Med Phys (40), 2013

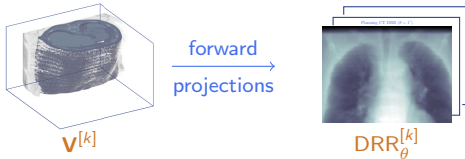
LIVE DTS algorithm¹



¹Zhang et al.
Med Phys (40), 2013

Iterative DRR-OBI registration

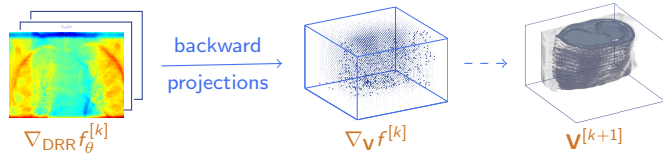
1. Digitally reconstructed radiographs (DRRs) for volume-image registration



2. Registration fidelity

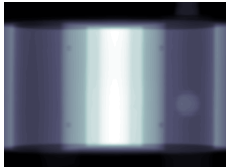
$$f \left(DRR_{\theta}^{[k]}, OBI_{\theta}^{[k]} \right) = \sum_{\theta} f_{\theta}^{[k]}$$

3. Deformation field estimate (DFE) update along pixel and voxel gradients

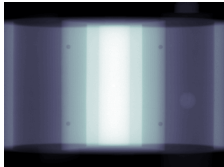


A glance at output and timing

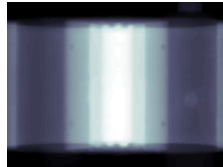
Planning CT DRR



OBI



DTS DRR



1m25s vs. 1h30m^{1,2}

6m22s

5m23s

¹Yan et al. *Medical Physics* (34), 2007

²Zhang et al. *Medical Physics* (40), 2013

Outline

1 Introduction: IGRT & LIVE

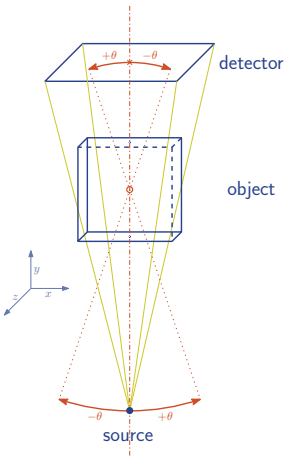
2 Cone-beam operators

3 Experiments

4 Discussion

5 Acknowledgements

Forward & backward cone-beam projections



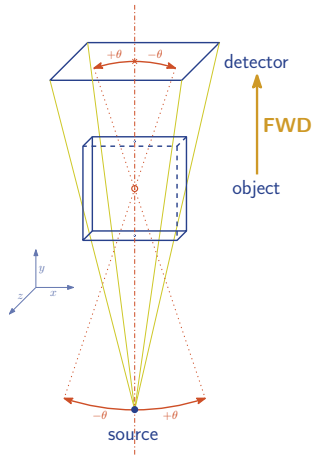
Staub & Murphy. *Medical Physics* (40), 2013

Feldkamp et al. *JOSAA* (1), 1984

Katsevich. *IJMMS* (21), 2003

Forward & backward cone-beam projections

- Forward projections: DRR generation
 - Volumetric ray-casting operator (primary effects)
 - Secondary effects (scatter, etc) beyond this talk



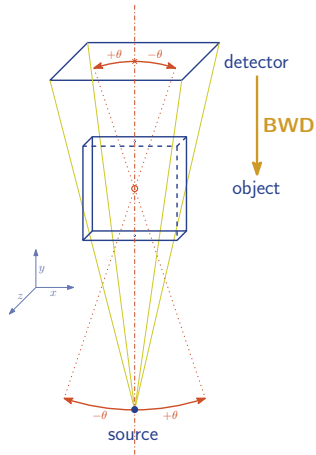
Staub & Murphy. *Medical Physics* (40), 2013

Feldkamp et al. *JOSAA* (1), 1984

Katsevich. *IJMMS* (21), 2003

Forward & backward cone-beam projections

- Forward projections: DRR generation
 - Volumetric ray-casting operator (primary effects)
 - Secondary effects (scatter, etc) beyond this talk
- Backward projections: DFE update
 - Filtered back-projection operator



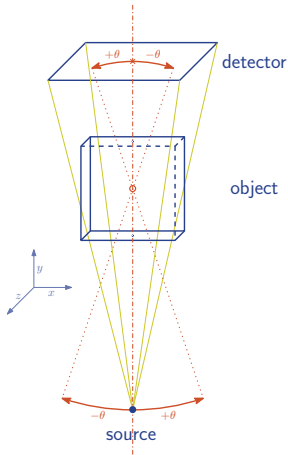
Staub & Murphy. *Medical Physics* (40), 2013

Feldkamp et al. *JOSAA* (1), 1984

Katsevich. *IJMMS* (21), 2003

Forward & backward cone-beam projections

- Forward projections: DRR generation
 - Volumetric ray-casting operator (primary effects)
 - Secondary effects (scatter, etc) beyond this talk
- Backward projections: DFE update
 - Filtered back-projection operator
- Clinical/DTS context
 - Fixed projection geometry
 - Processing within clinical response time (order of seconds)



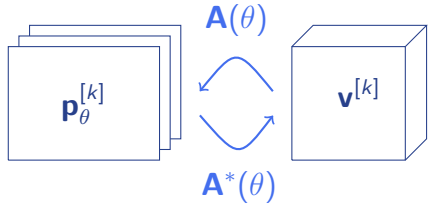
Staub & Murphy. *Medical Physics* (40), 2013

Feldkamp et al. *JOSAA* (1), 1984

Katsevich. *IJMMS* (21), 2003

A simple fact & a long battle

$$\mathbf{p}_\theta^{[k]} = \mathbf{A}(\theta) \mathbf{v}^{[k]}$$

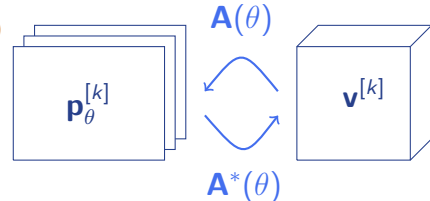


A simple fact & a long battle

projection operators
(fixed geometry)

$$\mathbf{p}_\theta^{[k]} = \mathbf{A}(\theta) \mathbf{v}^{[k]}$$

operands
(variable across iterations)



- $\{\mathbf{A}(\theta) \mid \theta \in \Theta\}$: pre-computable in theory
- Challenging in practice (past^{1,2} to present)
 - Memory capacity & communication bandwidth

¹Levoy. *PhD thesis*, UNC, 1989

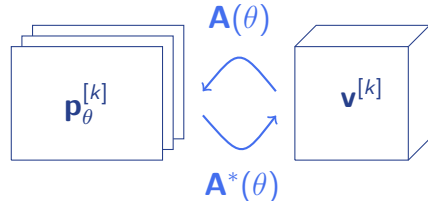
²Xu & Mueller. *IEEE TNS*, 2005

A simple fact & a long battle

projection operators
(fixed geometry)

$$\mathbf{p}_\theta^{[k]} = \mathbf{A}(\theta) \mathbf{v}^{[k]}$$

operands
(variable across iterations)



- $\{\mathbf{A}(\theta) \mid \theta \in \Theta\}$: pre-computable in theory
- Challenging in practice (past^{1,2} to present)
 - Memory capacity & communication bandwidth

N_v	N_p	N_Θ	$\tilde{N}_{\mathcal{R}}$	$S_{\mathcal{N}}$	Memory (GiB)
$256 \times 256 \times 160$	512×384	30	256	$2 \times 2 \times 2$	45.2
$256 \times 256 \times 160$	512×384	60	256	$2 \times 2 \times 2$	113.0
$512 \times 512 \times 320$	1024×768	60	512	$2 \times 2 \times 2$	903.8

¹Levoy. *PhD thesis*, UNC, 1989

²Xu & Mueller. *IEEE TNS*, 2005

Precursors and contribution

$$\mathbf{p}_\theta^{[k]} = \mathbf{A}(\theta) \mathbf{v}^{[k]}$$

θ -dependent & large 

- On-the-fly computations
 - HW/SW acceleration^{1,2,3,4,5}
 - Fourier-based methods^{6,7}
 - Ray/volume models^{8,9,10}
 - Fast ray descriptors^{11,12}
 - ...

$$\mathbf{p}_\theta^{[k]} = \mathbf{A}(0^\circ) \mathbf{B}(\theta) \mathbf{v}^{[k]}$$

- Lightweight pre-computations
 - Modest memory cost
- Fast on-line processing
 - Substantially reduced complexity
 - GPU-friendly

¹Nöel *et al.*, 2010

²Park *et al.*, 2011

³Dorgham *et al.*, 2011

⁴Jia *et al.*, 2012

⁵Marchelli *et al.*, 2013

⁶Lacroute & Levoy, 1994

⁷Choi *et al.*, 2014

⁸Mensmann *et al.*, 2011

⁹Gibou & Bertelli, 2012

¹⁰Fisher *et al.*, 2013

¹¹Siddon, 1985

¹²Gao, 2012

Precursors and contribution

$$\mathbf{p}_\theta^{[k]} = \mathbf{A}(\theta) \mathbf{v}^{[k]}$$

θ -dependent & large 

- On-the-fly computations
 - HW/SW acceleration^{1,2,3,4,5}
 - Fourier-based methods^{6,7}
 - Ray/volume models^{8,9,10}
 - Fast ray descriptors^{11,12}
 - ...

¹Nöel *et al*, 2010

³Dorgham *et al*, 2011

⁵Marchelli *et al*, 2013

⁷Choi *et al*, 2014

⁹Gibou & Bertelli, 2012

¹¹Siddon, 1985

²Park *et al*, 2011

⁴Jia *et al*, 2012

⁶Lacroute & Levoy, 1994

⁸Mensmann *et al*, 2011

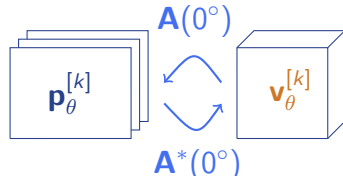
¹⁰Fisher *et al*, 2013

¹²Gao, 2012

$$\mathbf{p}_\theta^{[k]} = \mathbf{A}(0^\circ)(\mathbf{B}(\theta)\mathbf{v}_\theta^{[k]})$$

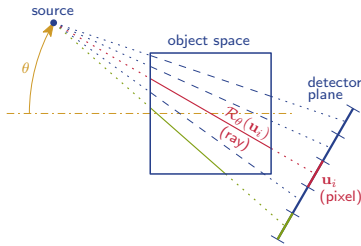
 compact
 θ -invariant

- Lightweight pre-computations
 - Modest memory cost
- Fast on-line processing
 - Substantially reduced complexity
 - GPU-friendly



Digital projection methods: **coupled** (object-centric)

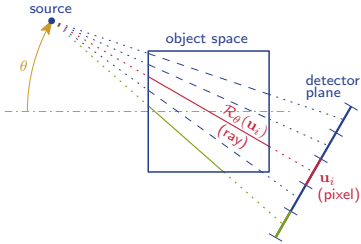
physical model



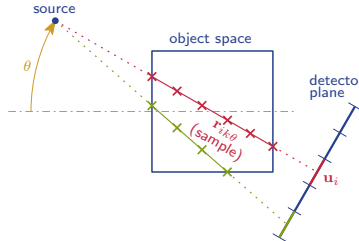
$$p_\theta^c(\mathbf{u}_i) = \int_{\mathcal{R}_\theta^c(\mathbf{u}_i)} v(\mathbf{u}_i, \rho) d\rho$$

Digital projection methods: **coupled** (object-centric)

physical model



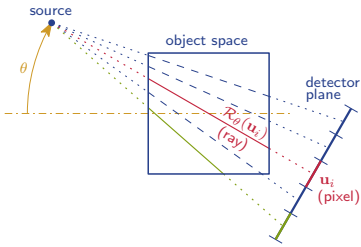
ray-grid sampling



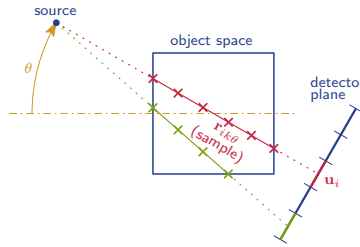
$$p_\theta^c(\mathbf{u}_i) = \int_{\mathcal{R}_\theta^c(\mathbf{u}_i)} v(\mathbf{u}_i, \rho) d\rho \quad p_\theta(\mathbf{u}_i) = \sum_{\rho_k \in \mathcal{R}_\theta(\mathbf{u}_i)} w_{ik\theta} v(\mathbf{r}_{ik\theta})$$

Digital projection methods: **coupled** (object-centric)

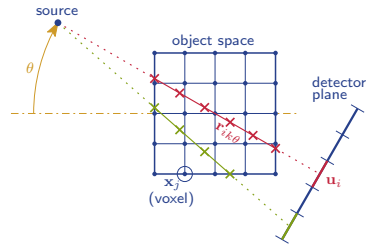
physical model



ray-grid sampling



Cartesian re-gridding



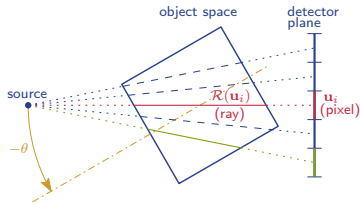
$$p_\theta^c(\mathbf{u}_i) = \int_{\mathcal{R}_\theta^c(\mathbf{u}_i)} v(\mathbf{u}_i, \rho) d\rho$$

$$p_\theta(\mathbf{u}_i) = \sum_{\rho_k \in \mathcal{R}_\theta(\mathbf{u}_i)} w_{ik\theta} v(\mathbf{r}_{ik\theta})$$

$$v(\mathbf{r}_{ik\theta}) \simeq \sum_{\mathbf{x}_j \in \mathcal{N}(\mathbf{r}_{ik\theta})} h_{ijk\theta} v(\mathbf{x}_j)$$

Digital projection methods: **factored** (gantry-centric)

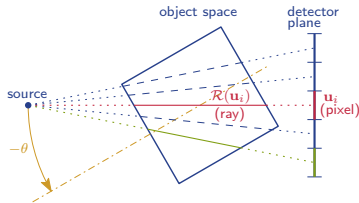
physical model



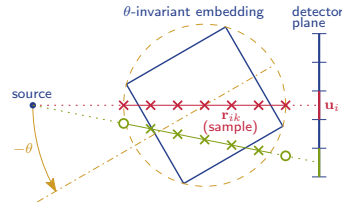
$$p_\theta^c(\mathbf{u}_i) = \int_{\mathcal{R}^c(\mathbf{u}_i)} v_\theta(\mathbf{u}_i, \rho) d\rho$$

Digital projection methods: **factored** (gantry-centric)

physical model



ray-grid sampling

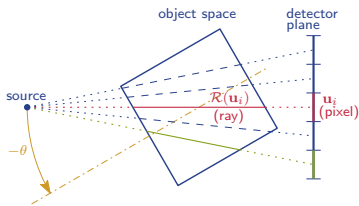


$$p_\theta^c(\mathbf{u}_i) = \int_{\mathcal{R}^c(\mathbf{u}_i)} v_\theta(\mathbf{u}_i, \rho) d\rho$$

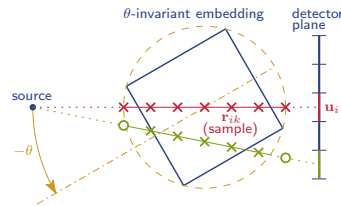
$$p_\theta(\mathbf{u}_i) = \sum_{\rho_k \in \mathcal{R}(\mathbf{u}_i)} w_{ik} v_\theta(\mathbf{r}_{ik})$$

Digital projection methods: **factored** (gantry-centric)

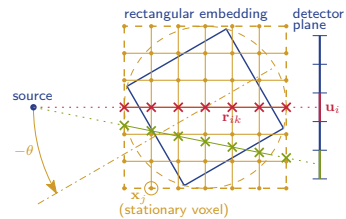
physical model



ray-grid sampling



Cartesian re-gridding



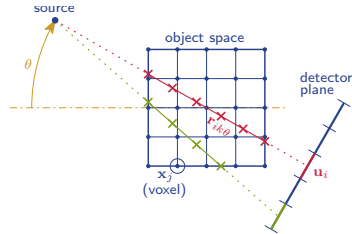
$$p_\theta^c(\mathbf{u}_i) = \int_{\mathcal{R}^c(\mathbf{u}_i)} v_\theta(\mathbf{u}_i, \rho) d\rho$$

$$p_\theta(\mathbf{u}_i) = \sum_{\rho_k \in \mathcal{R}(\mathbf{u}_i)} w_{ik} v_\theta(\mathbf{r}_{ik})$$

$$\begin{aligned} v_\theta(\mathbf{r}_{ik}) &\simeq \sum_{\mathbf{x}_j \in \mathcal{N}(\mathbf{r}_{ik})} h_{ijk}^{\text{ray}} \bar{v}_\theta(\mathbf{x}_j) \\ \bar{v}_\theta(\mathbf{x}_j) &\simeq \sum_{\mathbf{x}'_j \in \mathcal{N}_\theta(\mathbf{x}_j)} h_{jj'\theta}^{\text{traj}} v(\mathbf{x}'_j) \end{aligned}$$

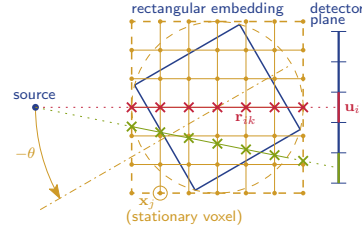
Digital projection methods: comparison

coupled



$$p_\theta(u_i) \simeq \sum_{r_{ik\theta} \in \mathcal{R}_\theta(u_i)} w_{ik\theta} \sum_{x_j \in \mathcal{N}(r_{ik\theta})} h_{ijk\theta} v(x_j)$$

factored

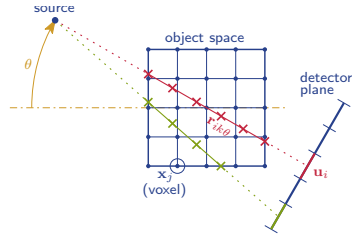


$$\bar{v}_\theta(x_j) \simeq \sum_{x'_j \in \mathcal{N}_\theta(x_j)} h_{jj'\theta}^{\text{traj}} v(x'_j)$$

$$p_\theta(u_i) \simeq \sum_{r_{ik} \in \mathcal{R}(u_i)} w_{ik} \sum_{x_j \in \mathcal{N}(r_{ik})} h_{ijk}^{\text{ray}} \bar{v}_\theta(x_j)$$

Digital projection methods: comparison

coupled

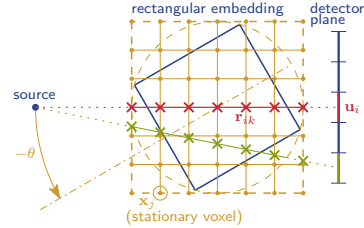


$$p_\theta(u_i) \simeq \sum_{r_{ik\theta} \in \mathcal{R}_\theta(u_i)} w_{ik\theta} \sum_{x_j \in \mathcal{N}(r_{ik\theta})} h_{ijk\theta} v(x_j)$$

$$\mathbf{p}_\theta \simeq \mathbf{C}(\theta) \mathbf{M}(\theta) \mathbf{v}$$

C: composite coefficients
M: geometric index mapping

factored

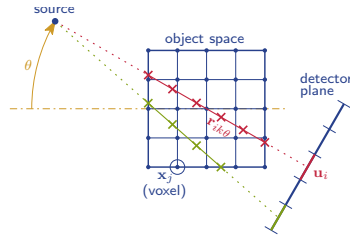


$$\begin{aligned} \bar{v}_\theta(x_j) &\simeq \sum_{x'_j \in \mathcal{N}_\theta(x_j)} h_{jj'\theta}^{\text{traj}} v(x'_j) \\ p_\theta(u_i) &\simeq \sum_{r_{ik} \in \mathcal{R}(u_i)} w_{ik} \sum_{x_j \in \mathcal{N}(r_{ik})} h_{ijk}^{\text{ray}} \bar{v}_\theta(x_j) \end{aligned}$$

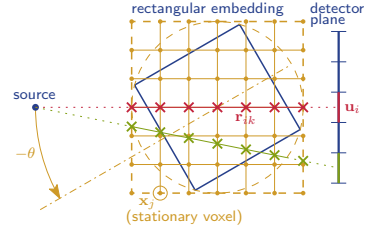
$$\begin{aligned} \bar{\mathbf{v}}_\theta &\simeq [(\mathbf{C}_{\text{traj}}(\theta) \mathbf{M}_{\text{traj}}(\theta)) \otimes \mathbf{I}_z] \mathbf{v} \\ \mathbf{p}_\theta &\simeq \mathbf{C}_{\text{ray}} \mathbf{M}_{\text{ray}} \bar{\mathbf{v}}_\theta \end{aligned}$$

Digital projection methods: comparison

coupled



factored



- θ -dependent ray projectors

- slice-invariant rotation
- θ -invariant ray projector

$$\mathbf{p}_\theta \simeq \mathbf{C}(\theta) \mathbf{M}(\theta) \mathbf{v}$$

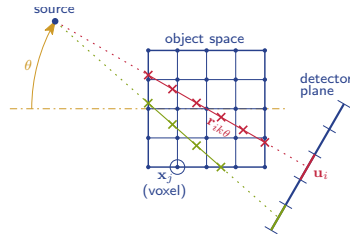
$\boxed{\begin{array}{l} \mathbf{C}: \text{composite coefficients} \\ \mathbf{M}: \text{geometric index mapping} \end{array}}$

$$\bar{\mathbf{v}}_\theta \simeq [(\mathbf{C}_{\text{traj}}(\theta) \mathbf{M}_{\text{traj}}(\theta)) \otimes \mathbf{I}_z] \mathbf{v}$$

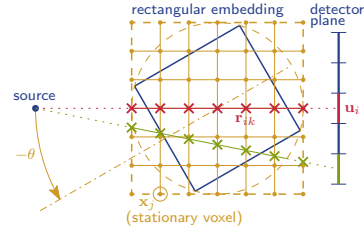
$$\mathbf{p}_\theta \simeq \mathbf{C}_{\text{ray}} \mathbf{M}_{\text{ray}} \bar{\mathbf{v}}_\theta$$

Digital projection methods: comparison

coupled



factored



- θ -dependent ray projectors
- one-step computations
- no embedding

- slice-invariant rotation
- θ -invariant ray projector
- up to 2 \times embedding domain size

$$\mathbf{p}_\theta \simeq \mathbf{C}(\theta) \mathbf{M}(\theta) \mathbf{v}$$

C: composite coefficients
M: geometric index mapping

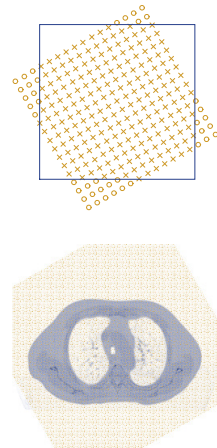
$$\bar{\mathbf{v}}_\theta \simeq [(\mathbf{C}_{\text{traj}}(\theta) \mathbf{M}_{\text{traj}}(\theta)) \otimes \mathbf{I}_z] \mathbf{v}$$

$$\mathbf{p}_\theta \simeq \mathbf{C}_{\text{ray}} \mathbf{M}_{\text{ray}} \bar{\mathbf{v}}_\theta$$

Re-composable operators

$$\mathbf{b} \simeq \mathbf{C} \mathbf{M} \mathbf{a}$$

- Static-dynamic decoupling
 - Pre-computed operators (**C** and **M**)
 - Simple computations with dynamic operands
- Flexible operator composition for improved accuracy
 - Ray projection (quadrature)¹
 - Regridding (interpolation kernel)²
- Additional potential for performance tuning
 - Known memory access patterns
 - Mapping to memory architecture (global/texture)



¹Engels. Academic Press, 1980

²Lehmann et al. IEEE TMI (18), 1999

Space and time complexities

Space (pre-computed coefficients)

- $M_{\text{oc}} = N_p \tilde{N}_{\mathcal{R}} N_{\Theta} S_{\mathcal{N}}$
- $M_{\text{gc}} = N_p \tilde{N}_{\mathcal{R}} S_{\mathcal{N}}^{\text{ray}} + N_v^{\text{xy}} N_{\Theta} S_{\mathcal{N}}^{\text{traj}}$

Time (online computations)

- T_{oc}
- T_{gc}

N_p : # of DRR pixels

$\tilde{N}_{\mathcal{R}}$: average # of samples per ray

N_{Θ} : # of projection angles

N_v : # of CT voxels

$S_{\mathcal{N}}$: neighborhood size of regridding kernel

same for helical and saddle source trajectories

Space and time complexities

Space (pre-computed coefficients)

- $M_{\text{oc}} = N_p \tilde{N}_{\mathcal{R}} N_{\Theta} S_{\mathcal{N}} = K_{\text{oc}}$
- $M_{\text{gc}} = N_p \tilde{N}_{\mathcal{R}} S_{\mathcal{N}}^{\text{ray}} + N_v^{\text{xy}} N_{\Theta} S_{\mathcal{N}}^{\text{traj}} = K_{\text{gc}}^{\text{ray}} + K_{\text{gc}}^{\text{traj}}$

Time (online computations)

- $T_{\text{oc}} = K_{\text{oc}}$
- $T_{\text{gc}} = K_{\text{gc}}^{\text{ray}} N_{\Theta} + K_{\text{gc}}^{\text{traj}} N_v^z$

N_p : # of DRR pixels
 $\tilde{N}_{\mathcal{R}}$: average # of samples per ray
 N_{Θ} : # of projection angles
 N_v : # of CT voxels
 $S_{\mathcal{N}}$: neighborhood size of regridding kernel

same for helical and saddle source trajectories

Space and time complexities

Space (pre-computed coefficients)

- $M_{\text{oc}} = N_p \tilde{N}_{\mathcal{R}} N_{\Theta} S_{\mathcal{N}} = K_{\text{oc}}$
- $M_{\text{gc}} = N_p \tilde{N}_{\mathcal{R}} S_{\mathcal{N}}^{\text{ray}} + N_v^{xy} N_{\Theta} S_{\mathcal{N}}^{\text{traj}} = K_{\text{gc}}^{\text{ray}} + K_{\text{gc}}^{\text{traj}}$

Time (online computations)

- $T_{\text{oc}} = K_{\text{oc}}$
- $T_{\text{gc}} = K_{\text{gc}}^{\text{ray}} N_{\Theta} + K_{\text{gc}}^{\text{traj}} N_v^z$

Set	Model settings					Space (GiB)		Time* (GFLOP)	
	N_v	N_p	N_{Θ}	$\tilde{N}_{\mathcal{R}}$	$S_{\mathcal{N}}$	O-C	G-C	O-C	G-C
A	$256 \times 256 \times 160$	512×384	30	256	$2 \times 2 \times 2$	45.2	1.2	23.0	9.8
B	$256 \times 256 \times 160$	512×384	60	256	$2 \times 2 \times 2$	113.0	1.3	26.7	19.6
C	$256 \times 256 \times 160$	512×384	60	256	$6 \times 6 \times 6$	244.2	3.4	805.6	206.1
D	$512 \times 512 \times 320$	1024×768	60	512	$2 \times 2 \times 2$	903.8	10.0	213.4	157.0

O-C: object-centric (coupled); G-C: gantry-centric (factored)

Outline

1 Introduction: IGRT & LIVE

2 Cone-beam operators

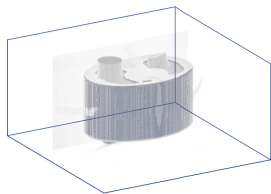
3 Experiments

4 Discussion

5 Acknowledgements

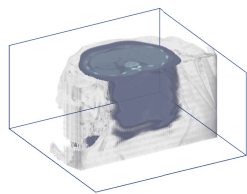
CT/OBI data-sets

(phantom)



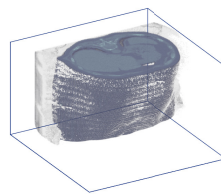
$256 \times 256 \times 136$

(patient 1)

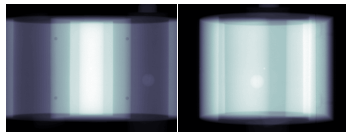


$256 \times 256 \times 136$

(patient 2)



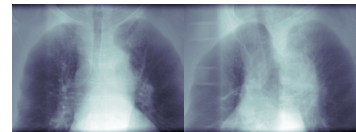
$256 \times 256 \times 166$



$(512 \times 384) \times 62$

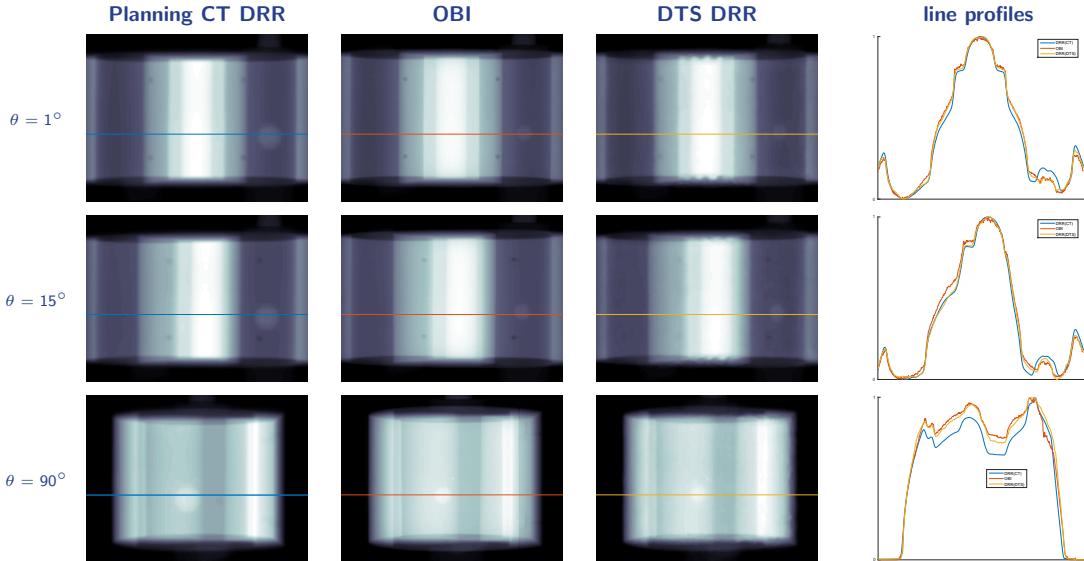


$(512 \times 384) \times 223$

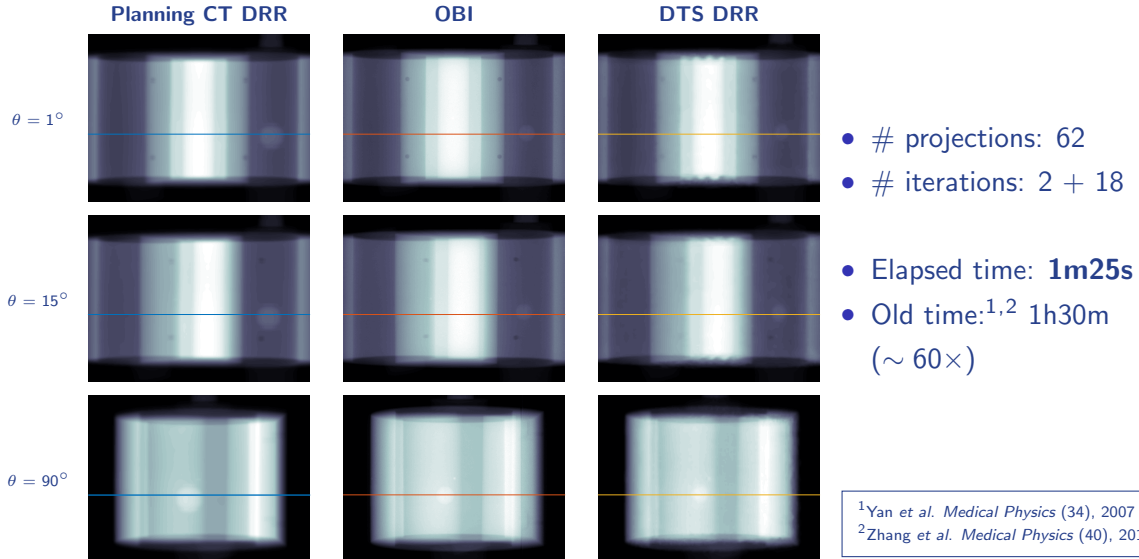


$(512 \times 384) \times 182$

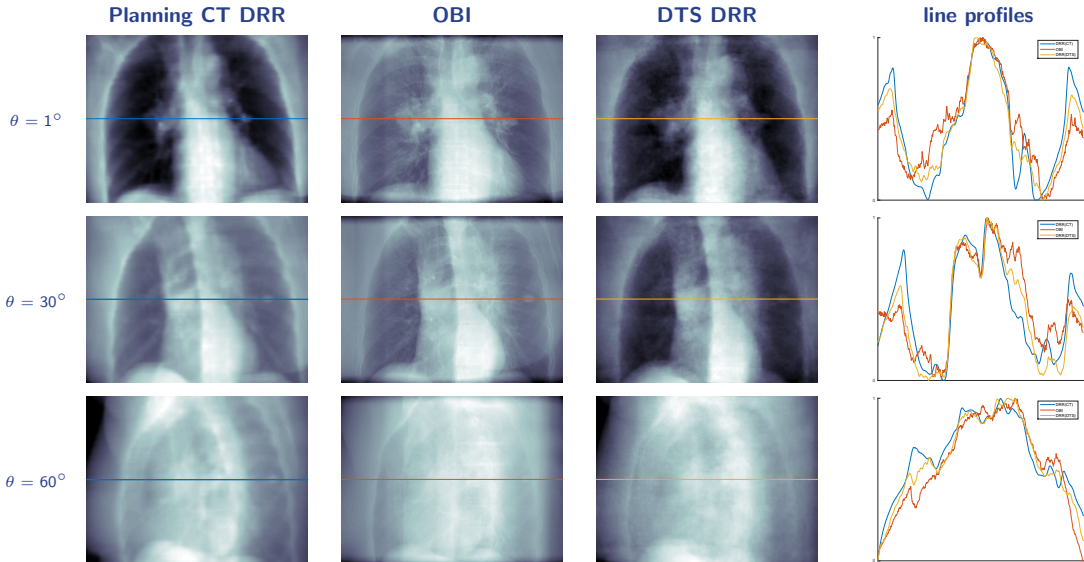
Results: phantom



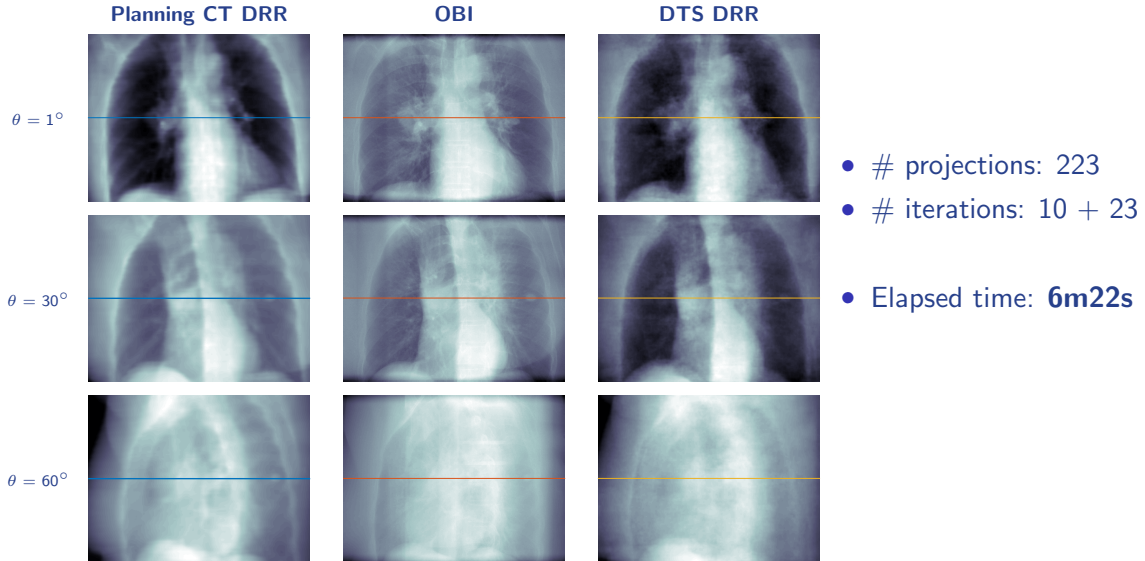
Results: phantom



Results: patient 1

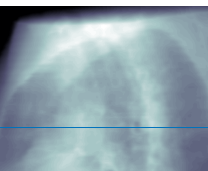
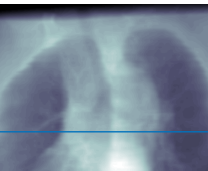
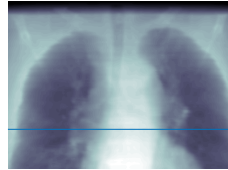


Results: patient 1

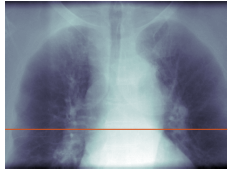


Results: patient 2

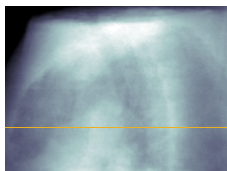
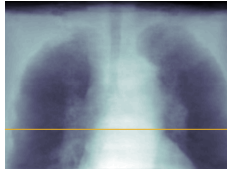
Planning CT DRR



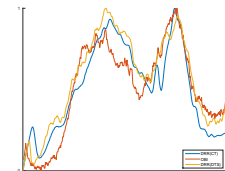
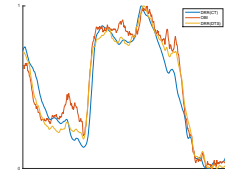
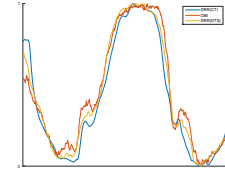
OBI



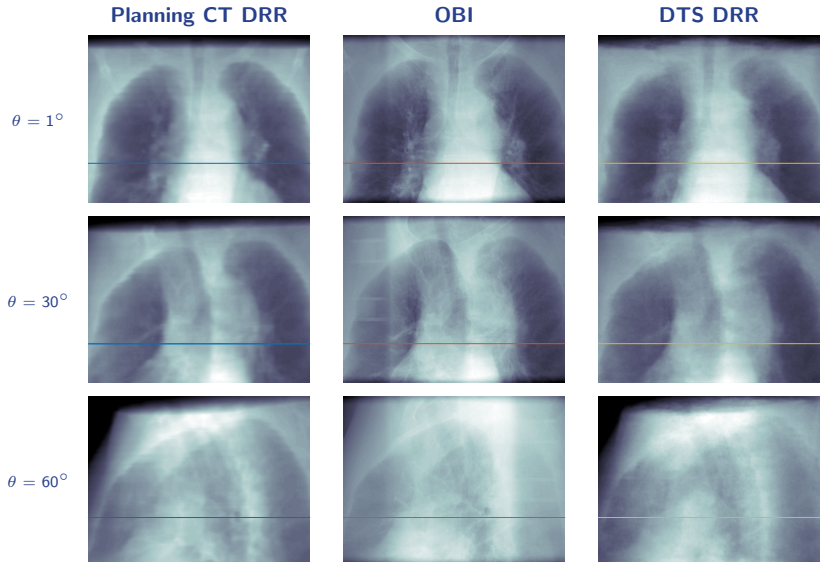
DTS DRR



line profiles



Results: patient 2



- # projections: 182
- # iterations: 10 + 20
- Elapsed time: **5m23s**

Outline

1 Introduction: IGRT & LIVE

2 Cone-beam operators

3 Experiments

4 Discussion

5 Acknowledgements

Recap & remaining challenges

- Re-composable operators: efficiency & flexibility without compromising accuracy
 - abstraction layer: research \longleftrightarrow performance
 - implementation acceleration still applicable
- Further directions:
 - numerical projector composition effect on iterations¹
 - planning-stage respiratory structure extraction/encoding²
 - memory access pattern optimization
 - algorithmic modifications (anatomical structure, low-contrast enhancement)
- LIVE is entering the clinical trials stage

¹ELEVIT 2015 (submission)

²AAPM Annual Meeting 2015 (submission)

Outline

- 1 Introduction: IGRT & LIVE
- 2 Cone-beam operators
- 3 Experiments
- 4 Discussion
- 5 Acknowledgements

Acknowledgements

- You Zhang
Medical Physics, Duke
- NIH Grant #R01-CA184173
- Lars Nyland
Senior Architect, NVIDIA
- ARO Grant #W911NF-13-I-0344
- Adjunct Associate Professor, UNC
K40 GPU donation, NVIDIA Corporation

Thank you!

contact: ailio@cs.duke.edu

References I

- [1] Z. Chang, J. Bowsher, J. Cai, S. Yoo, S. Wang, J. Adamson, L. Ren, and F.-F. Yin. Imaging system QA of a medical accelerator, novalis tx, for IGRT per TG 142: our 1 year experience. *Journal of Applied Clinical Medical Physics*, 13(4):113–140, Apr. 2012.
- [2] K. Choi, R. Li, H. Nam, and L. Xing. A Fourier-based compressed sensing technique for accelerated CT image reconstruction using first-order methods. *Physics in Medicine and Biology*, 59(12):3097–3119, June 2014.
- [3] O. Dorgham. *High speed 2D/3D medical image registration*. PhD thesis, University of East Anglia, Norwich, UK, June 2011.
- [4] H. Engels. *Numerical quadrature and cubature*. Computational mathematics and applications. Academic Press, 1980.
- [5] L. A. Feldkamp, L. C. Davis, and J. W. Kress. Practical cone-beam algorithm. *Journal of the Optical Society of America A*, 1(6):612, June 1984.

References II

- [6] M. Fisher, O. Dorgham, and S. D. Laycock. Fast reconstructed radiographs from octree-compressed volumetric data. *International Journal of Computer Assisted Radiology and Surgery*, 8(2):313–322, Mar. 2013.
- [7] H. Gao. Fast parallel algorithms for the x-ray transform and its adjoint. *Medical Physics*, 39(11):7110, Nov. 2012.
- [8] F. Gibou and L. Bertelli. Fast two dimensional to three dimensional registration of fluoroscopy and CT-scans using octrees on segmentation maps. *Mathematical Biosciences and Engineering*, 9(3):527–537, July 2012.
- [9] X. Jia, H. Yan, L. Cerviño, M. Folkerts, and S. B. Jiang. A GPU tool for efficient, accurate, and realistic simulation of cone beam CT projections. *Medical Physics*, 39(12):7368, Nov. 2012.
- [10] A. Katsevich. A general scheme for constructing inversion algorithms for cone beam CT. *International Journal of Mathematics and Mathematical Sciences*, 2003(21):1305–1321, 2003.
- [11] P. Lacroute and M. Levoy. Fast volume rendering using a shear-warp factorization of the viewing transformation. In *Proceedings of the 21st Annual Conference on Computer Graphics and Interactive Techniques*, SIGGRAPH '94, pages 451–458, Orlando, FL, USA, July 1994.

References III

- [12] T. M. Lehmann, C. Gönner, and K. Spitzer. Survey: Interpolation methods in medical image processing. *IEEE Transactions on Medical Imaging*, 18(11):1049–1075, Nov. 1999.
- [13] M. Levoy. *Display of Surfaces from Volume Data*. PhD thesis, Department of Computer Science, University of North Carolina at Chapel Hill, Chapel Hill, NC, USA, May 1989. TR89-022.
- [14] G. Marchelli, D. Haynor, W. Ledoux, R. Tsai, and D. Storti. A flexible toolkit for rapid GPU-based generation of DRRs for 2D-3D registration. In *Proceedings of SPIE*, volume 8669 of *Medical Imaging 2013: Image Processing*, page 86691C, Lake Buena Vista, FL, USA, Mar. 2013.
- [15] J. Maurer, T. Pan, and F.-F. Yin. Slow gantry rotation acquisition technique for on-board four-dimensional digital tomosynthesis. *Medical Physics*, 37(2):921, Jan. 2010.
- [16] J. Mensmann, T. Ropinski, and K. Hinrichs. Slab-based raycasting: Exploiting GPU computing for volume visualization. In *Computer Vision, Imaging and Computer Graphics. Theory and Applications*, volume 229, pages 246–259. Springer, Berlin, Heidelberg, 2011.
- [17] P. B. Noël, A. M. Walczak, J. Xu, J. J. Corso, K. R. Hoffmann, and S. Schafer. GPU-based cone beam computed tomography. *Computer Methods and Programs in Biomedicine*, 98(3):271–277, June 2010.

References IV

- [18] R. K. Panta, P. Segars, F.-F. Yin, and J. Cai. Establishing a framework to implement 4d XCAT phantom for 4d radiotherapy research. *Journal of Cancer Research and Therapeutics*, 8(4):565–570, 2012.
- [19] J. Park, S. Park, J. Kim, Y. Han, M. Cho, H. Kim, Z. Liu, Z. Jiang, B. Song, and W. Song. Ultra-fast digital tomosynthesis reconstruction using general-purpose GPU programming for image-guided radiation therapy. *Technology in Cancer Research and Treatment*, 10(4):295–306, Aug. 2011.
- [20] K. J. Redmond, D. Y. Song, J. L. Fox, J. Zhou, C. N. Rosenzweig, and E. Ford. Respiratory motion changes of lung tumors over the course of radiation therapy based on respiration-correlated four-dimensional computed tomography scans. *International Journal of Radiation Oncology*Biology*Physics*, 75(5):1605–1612, Dec. 2009.
- [21] L. Ren, I. J. Chetty, J. Zhang, J.-Y. Jin, Q. J. Wu, H. Yan, D. M. Brizel, W. R. Lee, B. Movsas, and F.-F. Yin. Development and clinical evaluation of a three-dimensional cone-beam computed tomography estimation method using a deformation field map. *International Journal of Radiation Oncology*Biology*Physics*, 82(5):1584–1593, Apr. 2012.

References V

- [22] L. Ren, Y. Zhang, and F.-F. Yin. A limited-angle intrafraction verification (LIVE) system for radiation therapy. *Medical Physics*, 41(2):020701, Feb. 2014.
- [23] R. L. Siddon. Fast calculation of the exact radiological path for a three-dimensional CT array. *Medical Physics*, 12(2):252, 1985.
- [24] R. Siegel, J. Ma, Z. Zou, and A. Jemal. Cancer statistics, 2014. *CA: A Cancer Journal for Clinicians*, 64(1):9–29, Jan. 2014.
- [25] D. Staub and M. J. Murphy. A digitally reconstructed radiograph algorithm calculated from first principles. *Medical Physics*, 40(1):011902, Jan. 2013.
- [26] G. J. Tornai, G. Cserey, and I. Pappas. Fast DRR generation for 2d to 3d registration on GPUs. *Medical Physics*, 39(8):4795, 2012.
- [27] L. Xing, B. Thorndyke, E. Schreibmann, Y. Yang, T.-F. Li, G.-Y. Kim, G. Luxton, and A. Koong. Overview of image-guided radiation therapy. *Medical Dosimetry*, 31(2):91–112, June 2006.
- [28] F. Xu and K. Mueller. Accelerating popular tomographic reconstruction algorithms on commodity PC graphics hardware. *IEEE Transactions on Nuclear Science*, 52(3):654–663, June 2005.

References VI

- [29] H. Yan, L. Ren, D. J. Godfrey, and F.-F. Yin. Accelerating reconstruction of reference digital tomosynthesis using graphics hardware. *Medical Physics*, 34(10):3768, Oct. 2007.
- [30] Y. Zhang, F.-F. Yin, W. P. Segars, and L. Ren. A technique for estimating 4D-CBCT using prior knowledge and limited-angle projections. *Medical Physics*, 40(12):121701, Nov. 2013.